Eur. J. Mineral., 38, 477–489, 2026
https://doi.org/10.5194/ejm-38-477-2026

European Journal of Mineralogy
Open Access

Preservation of water concentration in mantle xenoliths: a case study from Allègre and Ray Pic volcanoes (French Massif Central)

Konstantinos Thomaidis[1,2], Jannick Ingrin[1], Etienne Deloule[3], Lydéric France[3,4], and Huan Chen[5]

[1]Univ. Lille, CNRS, INRAE, Central Lille, UMR 8207, UMET – Unité Matériaux et Transformations, 59000 Lille, France
[2]Physical Science and Engineering Division, King Abdullah University of Science and Technology (KAUST), Thuwal 23955-6900, Saudi Arabia
[3]Université de Lorraine, CNRS, CRPG, 54000 Nancy, France
[4]Institut Universitaire de France (IUF), 75231 Paris, France
[5]College of Oceanography, Hohai University, Nanjing 210098, China

Correspondence: Konstantinos Thomaidis (konstantinos.thomaidis@kaust.edu.sa) and Jannick Ingrin (jannick.ingrin@univ-lille.fr)

Received: 28 November 2025 – Revised: 24 April 2026 – Accepted: 1 July 2026 – Published: 27 July 2026

Abstract. Water in the form of hydrous point defects in the crystal structure of pyroxenes from mantle xenoliths is frequently used to trace the water content in the lithospheric mantle. However, little is known about the mechanism that allows xenoliths to preserve deep hydrogen signatures and if we can avoid a complete or partial reset by reaction with the host magma during transport. In particular, it is unknown how much of the water content of xenoliths is modified during the emplacement of lava and cooling at the surface and by the eruption mode (effusive versus explosive). In this work, we attempted to address to these matters.

We analysed the water content of peridotite xenoliths from two localities in the French Massif Central, Allègre and Ray Pic, using Fourier transform infrared (FTIR) spectroscopy. We performed point analyses and profile measurements in olivine (ol), clinopyroxene (cpx), and orthopyroxene (opx) crystals derived from 17 xenoliths. The two localities have different types of outcrops. In Allègre, the xenoliths are present in a frozen lava lake with a vertical structure, while in Ray Pic, xenoliths are hosted both in pyroclastic deposits and in a lava flow running over more than 20 km along a riverbed. Both studies on xenoliths in different parts of the lava flow show that the solidification and cooling of the basalt at the surface do not significantly affect the water content of pyroxenes in the xenoliths. The xenoliths do not show the presence of diffusion profiles, and the water content is independent of the location of the xenoliths within the lava bodies. However, the comparison of the water content of xenoliths from the pyroclastic deposit and within the lava flow at Ray Pic shows that the water concentrations are strongly impacted by the degree of degassing of the magma before the eruption. The concentrations of xenoliths in the degassed lava flow are much lower, by a factor of > 10 in ol and ≥ 2 in cpx and opx, compared to xenoliths from the pyroclastic deposits. Therefore, water content measured in pyroxenes can only represent minimal values, even for xenoliths hosted in rapidly cooled volcanic products (e.g. explosive eruptions). The amount of water in mantle xenoliths does not reflect the original amount of water in the lithospheric mantle. On the contrary, this study indicates that xenoliths picked up within the same lava flow, even at a few metres' distance, can exhibit pyroxenes with different spectral signatures. This suggests that the spectral signatures have been acquired before the emplacement of the lava flow and were not affected by the late degassing that occurred just before the eruption of the lava flow.

1 Introduction

Peridotite xenoliths that are transported to the surface through volcanic processes provide a direct insight into the mineralogy and geochemistry of the upper mantle. They may also provide information on the concentration and speciation of water present in the lithosphere (e.g. Ingrin and Skogby, 2000; Grant et al., 2007; Demouchy and Bolfan-Casanova, 2016; Peslier et al., 2017). The wt ppm quantities of hydrogen incorporated as point defects in the crystal structure of the three main mantle minerals, olivine (ol), enstatite (opx), and diopside (cpx), have been extensively used to estimate the water speciation in the mantle lithosphere (Demouchy and Bolfan-Casanova, 2016; Peslier et al., 2017).

Pyroxenes are the most hydrous nominally anhydrous minerals (NAMs) in peridotite xenoliths. They dominate the water budget in the upper-mantle xenoliths, with concentrations ranging from 0 to 200 wt ppm H_2O for ol, 0 to 650 wt ppm H_2O for opx, and 0 to 1000 wt ppm H_2O for cpx (Bell and Rossman, 1992; Peslier, 2010; Demouchy and Bolfan-Casanova, 2016; Peslier et al., 2017).

The quantification of the water in the lithospheric mantle from xenoliths raises several questions. Water can be lost or added during the whole process of transport to the surface, from magma sampling of xenoliths to ascent, degassing, eruption, and cooling at the surface. The consensus is that pyroxenes are more trustworthy than ol for preserving information about the original water content of the mantle lithosphere (Denis et al., 2013; Tian et al., 2017). For instance, ol xenocrysts exhibit hydrogen diffusion profiles, whereas water concentration in pyroxenes is often homogenous (Demouchy et al., 2006; Peslier and Luhr, 2006). The water partition coefficient between pyroxenes is relatively constant, whereas it can vary over more than 1 order of magnitude for ol compared to pyroxenes (Grant et al., 2007; Demouchy and Bolfan-Casanova, 2016; Peslier et al., 2017). Nevertheless, hydrogen diffusion profiles have also been observed in pyroxenes from peridotites and granulite xenoliths, and a reset of water content during the late stage of their transport has been proposed (Tian et al., 2017; Denis et al., 2018; Li et al., 2024).

Experiments of hydrogen diffusion in pyroxenes generally point out toward a relatively fast diffusion at magma temperatures, suggesting that complete overprint of water concentration could occur in hours or days in pyroxenes (Ingrin and Blanchard, 2006; Farver, 2010; Ferriss et al., 2016; Demers-Roberge et al., 2021). However, hydrogen exchange rates vary strongly with pyroxene compositions (Ferriss et al., 2016; Yang et al., 2021). Moreover, all results are based solely on single-crystal experiments, and no convincing study has been conducted yet to understand how these findings can be extrapolated to a whole xenolith rock.

Therefore, the question of the kinetics of the equilibration of water content in xenoliths with magma and their ability to exchange during the different steps of their recovery from depth remains open.

In this study, we examine the impact of magma emplacement at the surface and its subsequent cooling on the water content of peridotite xenoliths in two basaltic volcanoes from the French Massif Central (FMC), Allègre and Ray Pic. Additionally, we examine the impact of the mode of eruption on the water content in Ray Pic. The water content of mantle xenoliths sampled in lava bodies from Allègre and Ray-Pic and from pyroclastic deposits from Ray-Pic volcanoes was investigated by Fourier transform infrared (FTIR) spectroscopy. The comparison of the water contents clearly shows that, even in the absence of evidence of diffusion profiles, the water content of xenoliths is easily modified during their transport to the surface. It cannot be used as it is to estimate the water content of the mantle lithosphere. The outcome is significant because it contradicts the conclusions drawn from over 2 decades of research.

2 Geological setting and samples

Alkali–basalt volcanoes have been active in the French Massif Central (FMC) since the early Cenozoic, with a peak at 4–6 Ma (Maury and Varet, 1980; Michon and Merle, 2001). The lithospheric mantle beneath the FMC and the related metasomatism processes that cause part of its compositional variability have been extensively studied (Lenoir et al., 2000; Wittig et al., 2007; Harvey et al., 2010; Bräuer et al., 2017; Uenver-Thiele et al., 2017). Based on mantle xenolith textural and geochemical characteristics, the FMC is divided into a northern and southern lithospheric domain, with a boundary located at 45°30′ N (Lenoir et al., 2000). The xenoliths studied in this work are hosted by Cenozoic alkali basalts that are located in the southern lithospheric domain. Samples are from two localities, Allègre in the Deves volcanic district and Ray Pic in the Velay Oriental volcanic district (Fig. S1 in the Supplement).

The first group of xenoliths originates from one single location, at the Ringue quarry in Allègre. The quarry cuts a thick basaltic body from the Allègre volcano, with a depth of more than 30 m. The lava body in Ringue quarry has been identified as part of a lava lake that filled a maar ~ 3 Ma ago (Ledru et al., 1994). Extensive prismatic jointing is exposed in the quarry, indicating the slow cooling of the magma body (Fig. S2). The samples were taken from the three different excavation levels (Fig. S2). Xenoliths from Allègre have been previously studied by Gu (Gu, 2016; Gu et al., 2016), who investigated water contents, trace elements in clinopyroxene, and Li concentrations and isotopic compositions in ol and pyroxenes. Their results suggest that the lithospheric mantle experienced multiple stages of cryptic metasomatism, likely related to carbonatitic melts and/or fluids or melts and/or fluids derived from subducted materials, as well as possible interaction with the host magma.

The second group of xenoliths was collected in the lava flow of the Ray Pic volcano, which follows La Bourges River, at various distances from the summit and from a maar deposit nearby the volcanic edifice (pyroclastic density current deposits; Fig. S3). The xenoliths from the pyroclastic deposits were sampled at the same location as those studied by Denis et al. (2015), situated along the road on the east flank of the volcano (Olivier Alard, personal communication, 2025). The geochemical and mineralogical composition of xenoliths from Ray Pic have been investigated in several previous studies (e.g. Downes and Dupuy, 1987; Zangana et al., 1997, 1999; Lenoir et al., 2000). The most recent extensive study is by Denis et al. (2015). It observed hydrous modal metasomatism marked by the presence of amphibole in 60 % of the xenoliths. Furthermore, cpx shows strong enrichments in highly incompatible elements when normalized to primitive mantle (PM) values (e.g. $(La/Sm)_{PM}$ up to 15.7) and negative anomalies in high-field-strength elements (e.g. $(Th/Nb)_{PM}$ up to ~ 680), consistently with carbonatitic metasomatism via small-volume volatile-rich melts. Despite the occurrence of amphibole, the water content of NAMs was not significantly affected, indicating that the hydrous metasomatism had no effect on the final water content of NAMs (Denis et al., 2015).

3 Methods

3.1 Samples

The xenoliths selected are classified as lherzolite (13), harzburgite (3), and dunite (1). The dominant texture present in the samples is protogranular, a granoblastic texture characterized by polygon-shaped grains and curvilinear mineral boundaries (Mercier and Nicolas, 1975). Several characteristics of the coarse granular and equigranular texture may be observed in some samples or exist as an intermediate or mixed texture. In the majority of the cases, we observe that (a) ol and opx are usually coarse grained and with similar size, (b) cpx is frequently of smaller size and often clustered with spinel, and (c) in most of the pyroxenes we observe exsolution textures. Pyro 2 is the only sample with a porphyroclastic texture. All samples have spinel as an accessory mineral. No evidence of deformation-induced orientation fabric was observed. There were no amphibole crystals visible in the samples that were analysed. The host magma of the xenoliths is a basalt with typical aphanitic-fine grained texture, with rare ol or pyroxene phenocrysts.

Petrological characteristics and phase chemical compositions of xenoliths from these two localities are reported in Gu et al. (2016) for Allègre and Denis et al. (2015) for Ray Pic. Gu et al. (2016) investigated xenoliths from the Allègre quarry and reported on their equilibrium temperatures and pressures. The values range between 840–1077 °C and 9.3–14.8 kbar based on the two-pyroxene thermometer and the Ca-in-olivine geobarometer of Brey and Köhler (1990). The same study reports major element composition, with Mg# varying between 89.2–92.4 for ol, between 89.6–92.9 for opx, and 88.5–92.7 for cpx.

Thin sections were prepared at the Geology department (University of Lille, France) and at the Thin Section Laboratory (Toul, France). The selected xenoliths, with sizes from 20 to 1500 cm^3, had fresh surfaces after breaking, with no evidence of weathering. We prepared, in total, 29 thin sections from 17 different xenoliths (6 from Allègre and 11 from Ray Pic) for infrared measurements. Residual resin was eliminated by acetone baths for over 24 h. The sections, with thicknesses ranging from 220 to 320 µm, were double polished. The final thickness of each section was measured to a precision of a few micrometres using a digital micrometre, and these measurements were used to normalize the spectral data.

3.2 Major and trace elements analysis of Ray-Pic basalt lava flow

Basalts hosting the xenoliths from the Ray Pic samples were analysed for major and trace elements to confirm their origin from the same basalt flow (Tables S1 and S2). The analyses were conducted at the SARM (Service d'Analyse des Roches et Minéraux), a national CNRS facility at CRPG (Nancy, France), using inductively coupled plasma mass spectrometry (ICP-MS iCapQ) and inductively coupled plasma optical emission spectroscopy (ICP-OES iCap6500) and following Carignan et al. (2001).

3.3 Fourier transform infrared spectroscopy (FTIR)

Unpolarized IR spectra were collected in transmitted light using a Bruker's Hyperion 3000 FTIR microscope coupled with a Vertex 70 spectrometer equipped with a single MCT detector at LASIRe laboratory (CNRS-University of Lille, France). Measurements were performed using a globar thermal light source and a KBr beam splitter. For each spectrum, 128 scans for the background and 256 scans for the sample were acquired in the wavenumber range of 600–4000 cm^{-1} with a resolution of 4 cm^{-1}. A 15× objective (100 × 100 µm analysis window) for single MCT analyses was used for analyses at the core of the grains (50 × 50 µm for profiles analyses). For each mineral phase in a xenolith, a representative spectrum was built by averaging the spectra collected in numerous grains (3 to 26 for ol; 3 to 35 for cpx; 5 to 67 for opx; see Tables 1 and 2 for details). The maximum absorbances of the OH bands were all largely below 0.3 as required by the method (Kovács et al., 2008). This prevents bias resulting from crystal orientation, ensuring that the measured OH concentrations and identified spectral signatures are accurately representative. Baseline subtraction was performed on the representative spectra using a polynomial function between 3130 ± 30 and 3790 ± 30 cm^{-1} for OH bands. Total absorbance of OH bands (A_{OH}) was calculated by integra-

tion over the wavenumber range of 3100 to 3800 cm^{-1}. All spectra were normalized by sample thickness in cm.

The OH concentration in pyroxenes was determined from the integral absorbance (A_{OH}) using the calibration by Bell et al. (1995). Error from the measurement of the integral absorbance, which is mainly due to uncertainty of the baseline modelling and subtraction, is between 10 %–20 % of the A_{OH}. This range of error was calculated by underestimating and overestimating the integral absorbance through two extreme possible baseline corrections (see example in Fig. S4). Water in ol from mantle xenoliths has bands in the infrared absorption spectrum in two regions, 3450–3700 and 3100–3450 cm^{-1}. We combined two calibrations for the calculation of the water content in ol: the bands in the high-frequency region over the window 3450–3600 cm^{-1}, using the calibration of Withers et al. (2012) and the bands in the low-frequency region over the window 3100–3450 cm^{-1}, using the general calibration of Libowitzky and Rossman (1997). We checked profiles in ol, cpx, and opx crystals in all thin sections except in sections from the Lep 4 sample.

4 Results

4.1 Water in Allègre xenoliths

We examined six xenoliths from Allègre, two from each excavation level of the quarry. The representative average spectra of cpx and opx are plotted in Fig. 1 for all samples. Most of the pyroxenes have the same spectral signature, with the most intense bands at the highest frequency (at 3600 cm^{-1} for opx and 3620 cm^{-1} for cpx). The cpx in sample 03 from level 2 has a slightly different signature, with the band at 3520 cm^{-1} being more intense than the band at 3620 cm^{-1}. However, since this spectrum was constructed from three individual spectra, it is insufficient to eliminate a potential effect of orientation on the relative intensity of the OH bands.

Water contents range from 126 to 194 wt ppm for cpx, from 30 to 55 wt ppm for opx, and < 1 wt ppm for ol (Table 1). The lithology does not seem to affect the water concentration of the pyroxenes and ol. The pyroxenes of the dunite and lherzolite samples of level 3 have comparable concentrations, while the two harzburgites from level 2 have different water concentrations (Table 1). The water concentration of cpx and opx fall within the restricted cpx / opx ratio (3–5), already observed in previous studies (Fig. 2; see, for instance, Demouchy and Bolfan-Casanova 2016). The values and the spectral signatures of the cpx and the opx are in good agreement with those reported by Gu (2016) (see Fig. 2). Allègre ol has a water content below the detection limit, which is around 1 wt ppm for the thickness of the thin sections (215 to 316 µm).

All the profiles measured within cpx and opx grains in the Allègre samples show a uniform water distribution (Fig. S5). Therefore, we conclude that water content is homogeneously distributed in all crystals and samples. While the absolute values of water content depend on the calibration method applied, our dataset is internally consistent and can reliably be used to assess how the location of xenoliths within the basaltic lava lake might affect their water content. The water concentration of pyroxenes is independent of the sampled level (Fig. 3) and remains relatively uniform throughout the entire magma body.

4.2 Water in Ray Pic xenoliths

For Ray Pic, we examined 11 xenoliths, 4 sampled from the pyroclastic deposit on the eastern flank of the volcanic edifice and 7 sampled along the basaltic flow at different distances from the volcanic centre (Fig. S3). All xenoliths are lherzolites except one (Lep 4), which is a harzburgite. The representative spectra of ol, cpx, and opx are plotted in Fig. 4. Pyroxenes in most samples have spectral signatures dominated by the band at high frequency, which is the most frequent signature observed in mantle xenoliths (the Type 1 of Azevedo-Vannson et al., 2021). Only two samples, Burz16 01 and Col 2, have different spectral signatures (Fig. 4). The band at 3525 cm^{-1} becomes dominant in cpx, and the doublet at 3570 and 3525 cm^{-1} becomes dominant in opx (the Type 2 of Azevedo-Vannson et al., 2021). The numbers of individual grains that were analysed are statistically relevant to avoid a bias of orientation (67 and 35 spectra in Burz16 01 and 17 and 4 spectra for Col 2 for opx and cpx, respectively). These particular band signatures have already been observed in several volcanoes. The end-member of the Type-2 signature has been identified in pyroxenite xenoliths from the FMC (Azevedo-Vannson et al., 2021). A progressive change in signature has also been observed among peridotite xenoliths from the volcanic field of Nógrád–Gömör (Patkó et al., 2019). The same dichotomy of signatures has also recently been reported for opx in mantle xenoliths from different sites in southern Patagonia in Argentina (Demers-Roberge et al., 2026).

Two small bands at 3685 and 3710 cm^{-1} can be seen in a number of cpx spectra (Fig. 4). They are clearly visible in three samples (Pyro 3, Pyro 4, Mon 1) and are suspected to be related to the presence of amphibole lamellae (Ingrin et al., 1989; Skogby et al., 1990). They are probably of pargasite composition, which has dominant OH bands at the same frequencies (Della Ventura et al., 2003). No macroscopic amphiboles were observed in the thin sections; however, the presence of pargasite lamellae is consistent with the macroscopic observation in some Ray Pic xenoliths studied by Denis et al. (2015). The same OH bands were also observed by these authors in one of the harzburgite studied (Denis et al., 2015; sample 13RP14).

Water contents range from 110 to 371 wt ppm H_2O for cpx, from 33 to 92 wt ppm H_2O for opx, and from 0.1 to 5.7 wt ppm H_2O for ol (Table 2). As for samples of Allègre, the water contents of cpx and opx fall within the restricted cpx / opx ratio (3–5; Fig. 5). The water content of ol is not

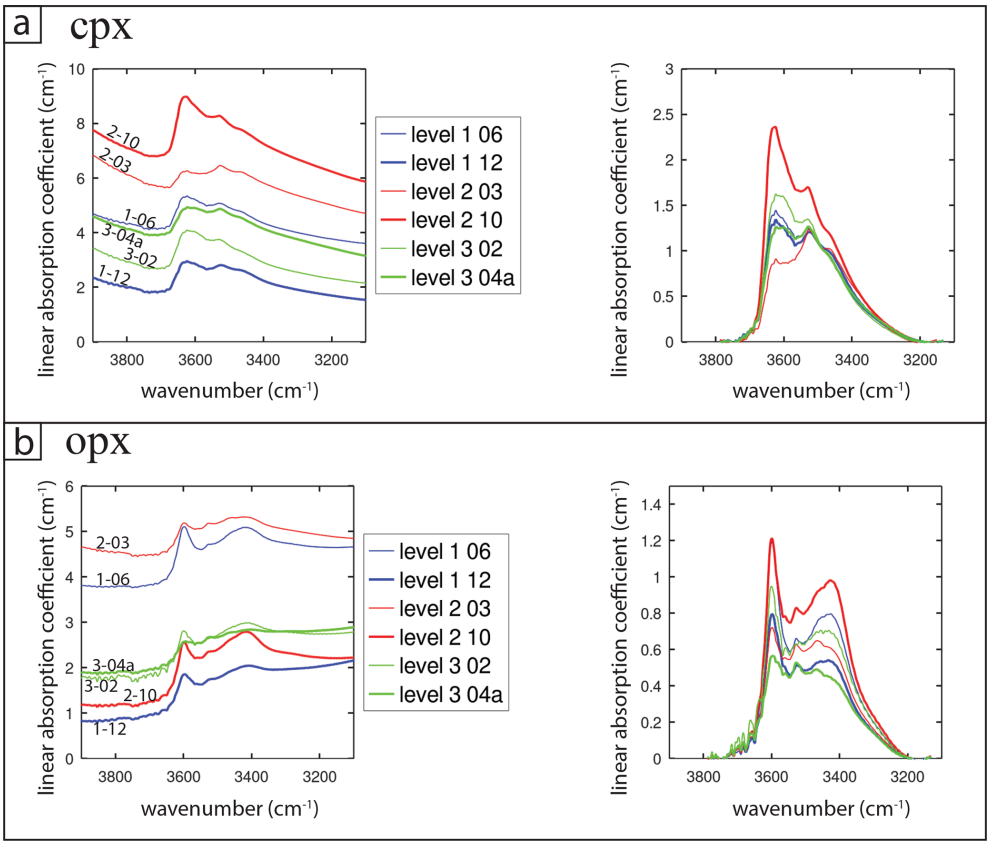

Figure 1. On the left, average **(a)** cpx and **(b)** opx infrared absorption spectra for Allègre xenoliths. On the right, corresponding A_{OH} integration area after baseline removal.

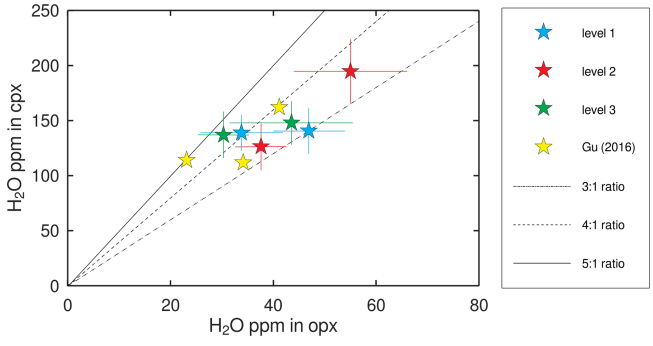

Figure 2. Water content in cpx versus opx in Allègre samples. Data from Gu (2016) are also plotted for comparison. Black lines show various cpx / opx correlation ratios.

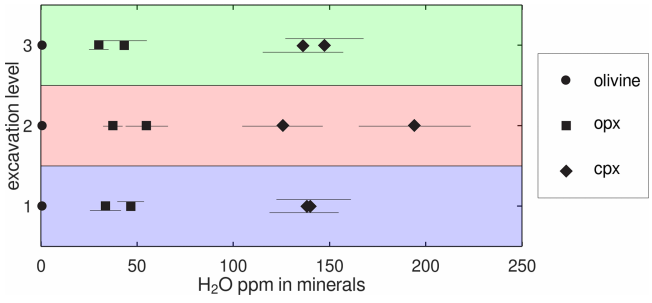

Figure 3. Plot of the H_2O wt ppm concentration in olivine and pyroxenes versus the excavation level.

correlated with the water content of pyroxenes. Water content from the xenoliths sampled in the pyroclastic products have systematically higher water content than xenoliths sampled within the lava flow (Table 2; Fig. 5).

The spectra of ol can be divided into two groups: (a) xenoliths from the pyroclastic deposits and (b) xenoliths from the basaltic lava flow. Xenoliths from the pyroclastic samples have a common signature with peaks at 3229, 3523, and 3573 cm^{-1} (Fig. 4), a signature akin to that of ol from Denis et al. (2015). The samples of group (b) have water concentrations below the detection limit (< 1 wt ppm H_2O), and no ol OH band was observed within the sections analysed. We specifically extracted and prepared six single olivine crystals from Burz16 01 to investigate the water content on thicker grains (thickness ranging from 3 to 6 mm). The Burz16 01 ol has a concentration of 0.10 $\pm$ 0.03 wt ppm H_2O. The representative average spectrum is plotted in Fig. 4. The signature of the spectrum is comparable to the one of ol from the py-

https://doi.org/10.5194/ejm-38-477-2026

Table 2. Ray Pic xenoliths: petrographic characteristics and water concentrations deduced from FTIR measurements. Total integral absorption (A_{OH}) and wt ppm H_2O values are rounded to the first decimal, and n denotes the number of different crystals used to calculate the average A_{OH}. All concentrations are in wt ppm H_2O. All profile measurements in ol, cpx, and opx crystals from Ray Pic samples were flat. The first part of the table is for the samples from the pyroclastic deposit, and the second part is for the samples from the basaltic flow.

Ray Pic sample	Distance (km)	Lithology	Mineral proportions				Texture	Ol			Cpx			Opx			cpx / opx ratio
			ol	cpx	opx	sp		n	A_{OH} (cm^{-2})	ppm	n	A_{OH} (cm^{-2})	ppm	n	A_{OH} (cm^{-2})	ppm	
Pyro 1	0	Lherzolite	56	10	31	3	prg	3	30.7	5.7 ± 0.4	5	876.6	370.9 ± 32	13	346.7	70.1 ± 9	5.3
Pyro 2	0	Lherzolite	46	14	36	4	prc	3	8.6	1.7 ± 0.1	12	842.6	356.5 ± 40	8	355.4	71.8 ± 6	5.0
Pyro 3	0	Lherzolite	44	12	40	4	prg	8	6.6	1.3 ± 0.2	9	861.1	364.4 ± 27	10	456.9	92.4 ± 9	3.9
Pyro 4	0	Lherzolite	53	6	38	3	prg	5	9.8	1.9 ± 0.1	12	782.8	331.2 ± 32	12	439.6	88.9 ± 11	3.7
RayPic16 02	0	Lherzolite	62	6	29	3	prg	12		< 1	15	500.1	211.6 ± 38	41	229.2	46.3 ± 11	4.6
RayPic16 04	0	Lherzolite	58	8	32	2	prg	5		< 1	5	548.7	232.2 ± 30	5	274.7	55.5 ± 11	4.2
Lep 4	5.3	Harzburgite	78	2	16	4	prg	12		< 1	–	–	–	27	187.6	37.9 ± 4	–
Burz16 01	9.2	Lherzolite	50	10	37	3	prg	6	0.56	0.10 ± 0.03	35	451.9	191.2 ± 22	67	289.2	58.5 ± 12	3.3
Burz16 02	9.2	Lherzolite	68	12	16	4	prg	26		< 1	16	349.8	148.0 ± 10	21	163.5	33.0 ± 6	4.5
Mon 1	11.9	Lherzolite	65	7	24	4	prg	6		< 1	9	614.4	260.0 ± 23	14	248.7	50.3 ± 5	5.2
Col 2	12.9	Lherzolite	58	7	32	3	prg	6		< 1	4	261.2	110.5 ± 12	17	163.5	33.1 ± 4	3.3

Note that sp denotes spinel, prg denotes protogranular, prc denotes porphyroclastic; < 1 wt ppm H_2O for ol corresponds to the detection limit.

Table 1. Allègre xenoliths: petrographic characteristics and water concentrations deduced from FTIR measurements. Total integral absorption (A_{OH}) and wt ppm H_2O values are rounded to the first decimal, and n denotes the number of different crystals used to calculate the average A_{OH}. All concentrations are in wt ppm H_2O.

Allègre sample	Lithology	Mineral proportions				Texture	Ol			Cpx			Opx			cpx / opx
		ol	cpx	opx	sp		n	A_{OH} (cm^{-2})	wt ppm	n	A_{OH} (cm^{-2})	wt ppm	n	A_{OH} (cm^{-2})	wt ppm	ratio
Level 1 06	Lherzolite	57	7	33	3	prg	3		< 1	21	330.8	140.0 ± 21	18	231.0	46.7 ± 7	3.0
Level 1 12	Lherzolite	53	14	29	4	prg	12		< 1	30	327.3	138.5 ± 16	26	166.3	33.6 ± 8	4.1
Level 2 03	Harzburgite	73	4	22	1	prg	11		< 1	4	297.2	125.7 ± 21	25	184.8	37.4 ± 5	3.4
Level 2 10	Harzburgite	77	3	19	1	prg	11		< 1	14	458.8	194.1 ± 29	17	271.0	54.8 ± 11	3.5
Level 3 02	Dunite	92	2	4	2	prg	9		< 1	3	348.4	147.4 ± 20	6	214.0	43.3 ± 12	3.4
Level 3 04a	Lherzolite	42	12	42	4	prg	10		< 1	27	322.2	136.3 ± 21	44	148.8	30.1 ± 5	4.5

Note that sp denotes spinel, and prg denotes protogranular.

roclastic deposits, but with a much smaller linear absorption of the bands.

The plot of water concentrations as a function of the distance from the source of the basalt flow shows no clear correlation (Fig. 6). It shows that the water content of opx from the basalt remains relatively constant all along the valley. Samples from RayPic16 02, Lep 4, Burz16 01, Burz16 02, Mon 1, and Col 2 for opx and RayPic16 02, Burz16 01, Burz16 02, and Mon 1 for cpx have average concentrations of 43.2 and 202.7 wt ppm H_2O for opx and cpx, respectively. The dispersion of data is low for opx and cpx, close to the value of individual error bars. All concentration values of ol from the lava flow have much less than 1 wt ppm H_2O.

The water contents reported in Denis et al. (2015) are 335–623 wt ppm H_2O for cpx and 68–171 wt ppm H_2O for opx. Even though our measurements in the pyroclastic samples are in the lower range of Denis et al. (2015), they are comparable (Fig. 5). Nevertheless, the range of water concentration in pyroxenes can vary up to a factor of 2 within these samples (Fig. 5).

5 Discussion

5.1 Allègre – a cross-section through a lava lake

Our study aims to identify the potential impact of magma degassing during surface emplacement on the water content of NAMs. Results presented in the Fig. 3 suggest that the water content of pyroxenes does not have any clear correlation with the sampling level of the xenolith within the fossil lava lake.

The solidification time of a basalt body 10 to 30 m thick can vary with the boundary conditions, but it generally takes several years, with a slow temperature decrease after solidification (less than 50 °C per year, Shaw et al., 1977; Peck, 1978; Wittmann et al., 2017; Philpotts and Ague, 2018). We observed a progressive disorganization of the well-defined columnar structure of the basalt from the bottom of the quarry at level 1 toward levels 2 and 3, with columnar structure disappearance at the top of level 3 (Fig. S2). This is in agreement with a faster cooling toward the top surface of the body. The cooling rate in level 1 and 2 was thus likely to be significantly lower than the one in level 3. Nevertheless, the water concentration of pyroxenes in xenoliths is independent of the position of the xenolith in the frozen lava lake. It means that the water concentration was not affected by the differences in the cooling rate of the magma body during its solidification. The absence of diffusion profiles, at least at the scale of the performed analyses (50–100 µm), is also an argument against a major reset of water content at this stage of the volcano history. Indeed, any partial reset of the water content of the pyroxenes in the xenoliths during solidification would have left evidence at the crystal scale through profiles in the pyroxenes due to the very progressive cooling of the solidified body. Although not related to sampling level, inter-sample water content heterogeneity is observed in the studied xenoliths (e.g. sample 03: 125.7 and 37.4 wt ppm H_2O for cpx and opx, respectively; sample 10: 194.1 and 54.8 wt ppm H_2O for cpx and opx, respectively). This heterogeneity, unrelated to sampling location, therefore highlights that the water content heterogeneity was acquired before xenolith emplacement within the lava lake and its progressive solidification. Water content heterogeneity of pyroxenes thus records either early lithospheric processes (e.g. partial melting, hydrous or carbonatitic metasomatism) or xenolith interactions with host magma during magma percolation at depth and subsequent ascent to the surface. The inherited heterogeneity is undoubtedly associated with the chemical heterogeneity of point defects in pyroxenes, which is a combination of vacancies, substitutions, and interstitials. However, due to the intricate and multifaceted relationships between point defects and major and trace elements, a clear correlation between the composition of xenoliths and water content has rarely been observed (see, for instance, the reviews by Peslier, 2010; Demouchy and Bolfan-Casanova, 2016). For instance, experimental studies have shown a positive correlation between the Al content of opx in equilibrium with a water-rich melt (Hauri et al., 2006). Experiments have also shown that ^{IV}Al in cpx phenocrysts is directly correlated with the water content of cpx in equilibrium with the melt (O'Leary et al., 2010). This has been effectively observed in natural phenocrysts. However, these correlations are rarely observed in opx or cpx from spinel peridotite xenoliths, which are not in chemical equilibrium with the host magma. Even the most recent attempts to explain the water partitioning between cpx and opx in xenoliths from the composition of major elements have failed (see, for instance, Ju et al., 2025). In the specific case of Allegre and Ray-Pic, previous studies have proved that there is no obvious correlation between the water content and Al content of pyroxenes (Gu, 2016; Denis et al., 2015, respectively; Table S3).

As magma ascent timescales from superficial magma chambers are usually in the range of hours to weeks (Moussallam et al., 2019; Elms et al., 2023), thus being clearly shorter than the cooling duration of thick lava flows or lava lakes, it is highly unlikely that the water content heterogeneity in pyroxenes is related to this xenolith transport stage; it more probably reflects the water content of pyroxenes in the magma chamber just before eruption.

5.2 Ray Pic – evolution along a basalt lava flow and in the pyroclastic deposit

5.2.1 Samples from the basalt flow

Basalt samples from the lava flow were collected in a well-marked prismatic structure for samples RayPic16, Burz16, and Mon, while samples Lep and Col were collected in lava flow sections where the prismatic structure is less visible. This suggests that the latter two samples were collected in a part of the lava flow that had suffered a slightly different

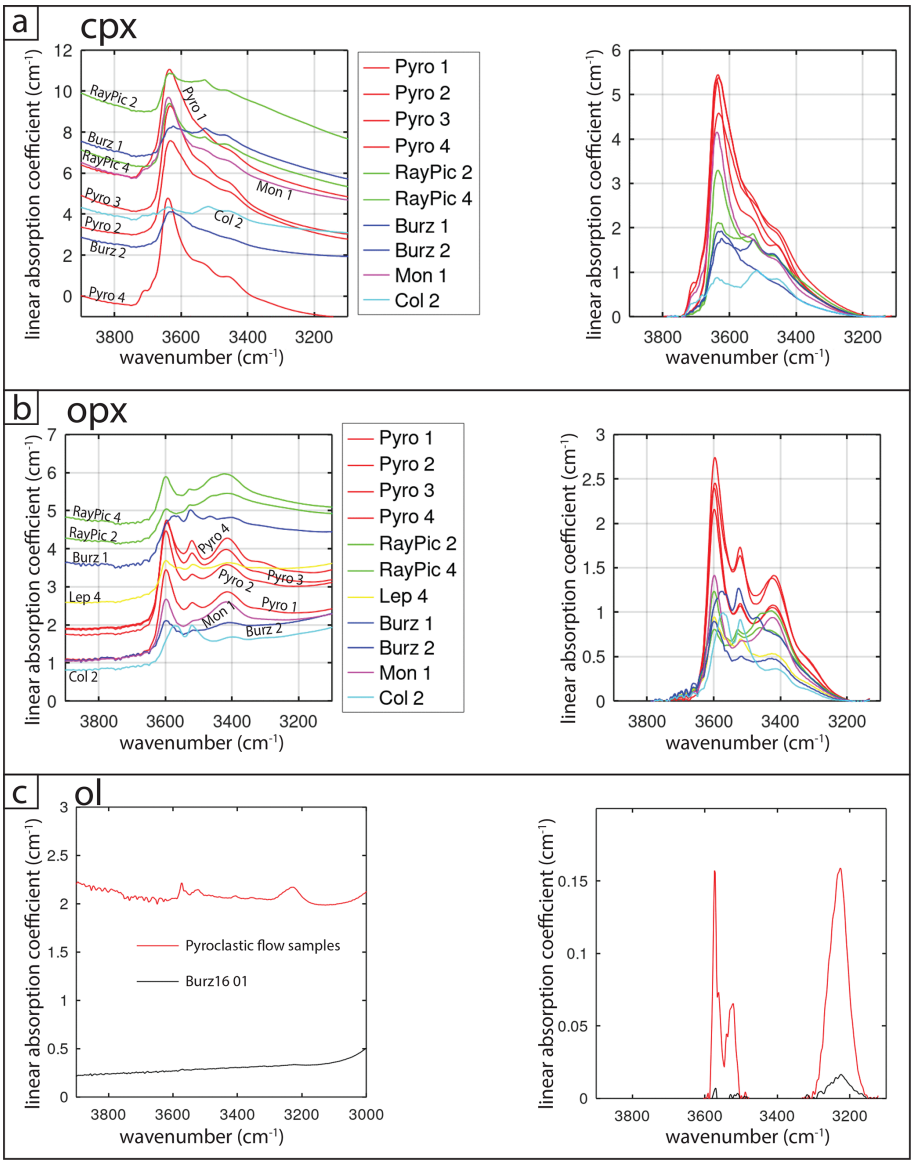

Figure 4. Average representative cpx, opx, and ol spectra for the Ray Pic xenoliths. On the right, corresponding A_{OH} integration area after baseline removal. For ol we plotted the average spectra from all pyroclastic flow samples (four samples) and the one from the six olivine crystals of sample Burz16 01 for the basaltic flow.

cooling rate. However, the water content of opx in the Lep sample was not significantly different compared to the ones of other samples from the lava flow with the same type of signature. Due to the small size of the opx it was not possible to measure profiles in this sample. Nevertheless, considering the data collected, there is no evidence that the samples from these two outcrops had kept more water compared to the others. The lower concentration observed in the sample from Col could be attributed to the difference in spectral signature. It has already been reported that such signatures have a tendency to be associated with lower water concentrations (Patkó et al., 2019).

Therefore, there is no clear trend in the evolution of the water content of xenoliths with the distance from the source of the lava flow or with the location inside the basalt flow (Fig. 6). This result is consistent with what we observed in the case of Allègre. The history of emplacement and solidification of basalt bodies does not significantly alter the water content of pyroxenes acquired prior to the eruption.

5.2.2 Samples from the pyroclastic deposit

On the contrary, the difference between samples from the lava flow and from the pyroclastic deposits is evident. The water concentrations of pyroxenes from the xenoliths hosted

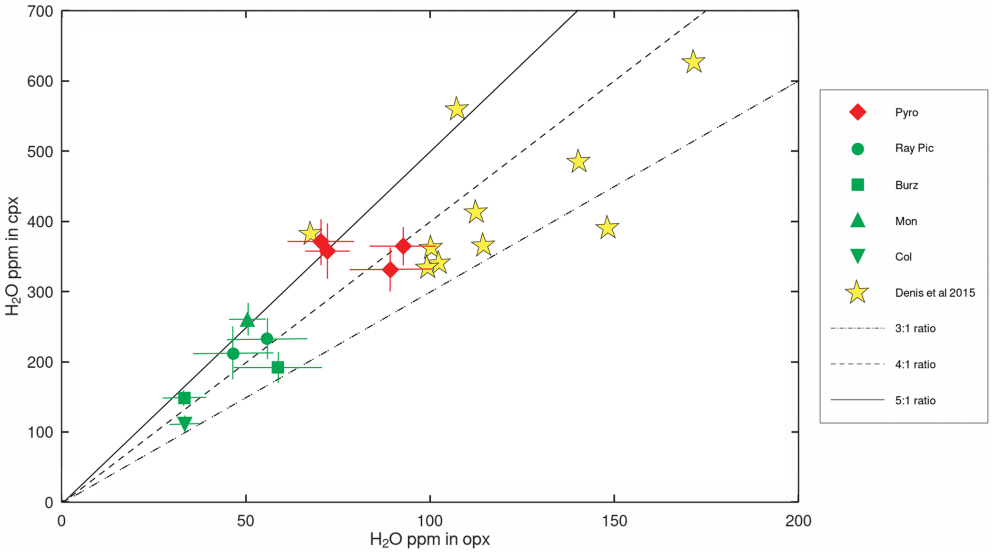

Figure 5. Water content in cpx versus opx in Ray Pic samples. Data from Denis et al. (2015) are also plotted for comparison. Black lines show various cpx / opx correlation ratios.

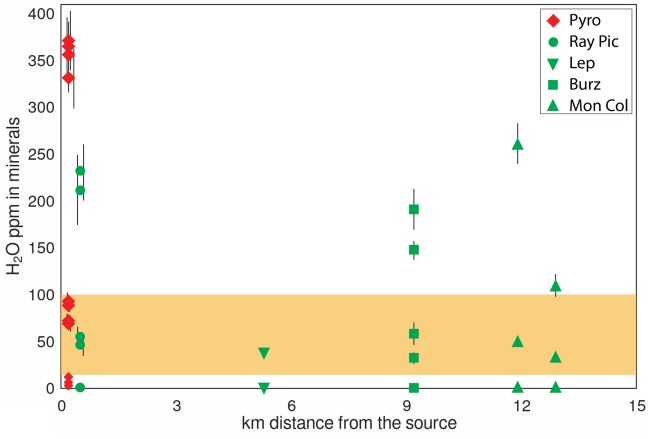

Figure 6. Plot of the wt ppm H_2O concentration in ol, opx, and cpx versus the distance from the source. Ol samples are below the orange area, opx samples are within, and cpx samples are above. Pyro and Ray Pic samples are spaced apart so that they are visible and do not overlap.

in the pyroclastic deposits are more than 50 % higher than the ones from the basalt lava flow. The depletion of water in ol from the xenoliths hosted in the basalt lava flow compared to those from the pyroclastic deposits is even stronger. The two events were sub-contemporaneous, and the hydration of the lithospheric mantle below has certainly not changed between the two events. Therefore, we can conclude that the xenoliths in the basalt lava flow had lost part of their water and were re-equilibrated at lower water fugacity than the xenoliths from the pyroclastic deposit. The final water content of the xenoliths has not been significantly affected by the emplacement of the basalt lava flow and its cooling after solidification, as we previously observed in the case of the Allègre lava lake. The modification of the water content of the pyroxenes is most probably due to an exchange with the magma before the eruption in a superficial magma chamber. It is frequently argued that the sampling of xenoliths among pyroclastic is more reliable than in basalt flow because the former is more rapidly quenched than the latter. Our study indicates that the effect of basalt cooling on the water content of xenoliths is limited. This points to another explanation for the origin of the difference between the two sets of data: a complete re-equilibration with a largely degassed magma just prior to the eruption for the xenoliths embedded in the lava flow (no profiles observed) and a re-equilibration with a less degassed magma for the xenoliths in the pyroclastic deposit. The two sets of xenoliths record re-equilibration in superficial magma chambers just before the eruptions. The effusive nature of the basalt flow compared to the explosive one that characterizes production of pyroclastic products is generally a sign of a more degassed magma, and its impact on the water content of the xenoliths is clear in the case of Ray Pic. Xenoliths can reside for days to years in a crustal magma chamber before being rapidly transferred to the surface (Moussallam et al., 2019). This is enough time to allow a full re-equilibration of the xenoliths with the magma. Even xenoliths sampled in products from explosive eruptions may have been re-equilibrated with a magma that was already partially degassed. The wide range of water concentrations in the pyroxenes of Ray Pic from the study of Denis et al. (2015), up to a factor of 2, shows that various degrees of magma degassing can be recorded by xenoliths even when sampled during an explosive event.

A direct consequence of these observations is that a complete re-equilibration of the water content of xenoliths can

easily occur before and during the eruptive sequences of a volcano. The water content of the magma settled in the crust may evolve during the eruption cycle of a volcano. Even xenoliths sampled in products from explosive eruptions may have re-equilibrated with a magma that was already partially degassed. Consequently, data collected from xenoliths represent only a lower limit of the water content of the xenolith in equilibrium with the host magma at the lithosphere depth of the sampling. This result is in perfect agreement with the observations and conclusion of the recent paper by Demers-Roberge et al. (2026), suggesting that the original water content of xenoliths was modified upon ascent. It also explains why a direct correlation of the water content of pyroxenes with their composition, pressure, and temperature of origin was rarely observed.

Despite this strong limitation, the observation of different spectral signatures in Col 2 and Burz16 01 pyroxenes raises hope for the use of OH infrared spectroscopy in the study of water in xenoliths. It suggests that, despite the slow cooling of the basalt flow and a re-equilibration of the total water content of the xenoliths in the magma chambers, before the eruption, the initial difference in the spectral signatures of pyroxenes may have not been erased. Samples with different spectral signatures can coexist within the same lava flow at a few metres' distance, as for the samples Burz16 01 and 02. Spectral signatures may be inherited from equilibration acquired before the degassing of the magma, possibly at mantle depth. Demers-Roberge et al. (2026) attribute the difference in the spectral signatures of pyroxenes to two possible explanations: (1) a deep origin which has not yet been identified because "too many processes or parameters were involved at the same time" and (2) a late "crystal-scale process" occurring during the slow cooling of the lava flows after emplacement that transforms the Type-1 spectral signature into a Type 2. As argued by Demers-Roberge et al. (2026), the observation of the signature of Type 2, mostly in xenoliths hosted in lava flow, favours the latter interpretation. However, this interpretation does not explain why most of the xenoliths in the thick lava flows of Allègre and Ray Pic have not been affected. It also does not explain why the two signatures can be observed in nearby xenoliths in the same body, as in Ray Pic. Another issue is that it is difficult to reconcile the fact that the Type-1 signature predates Type 2 with the observation of the opx crystals with a dominant signature of Type 1 at the rim and of Type 2 in the core (Demers-Roberge et al., 2026). As a last point, the change in the OH spectral signature generally modifies both pyroxenes simultaneously (see, for instance, Patkó et al., 2019; Azevedo-Vannson et al., 2021; Demers-Roberge et al., 2026). Consequently, it remains difficult to explain why clinopyroxene phenocrysts in the lava flows systematically exhibit a Type-1 signature (Huan Chen personal communication; Xia et al., 2013; Chen et al., 2015; Liu et al., 2015). Finally, the origin of the OH spectral signature of Type 2 in pyroxenes, whether it occurred prior to degassing or subsequent to emplacement, remains a topic of debate.

6 Conclusions and outlook

First, the study of xenoliths from the frozen lava lake in Allègre and along the 20 km basalt flow at Ray Pic shows that solidification and cooling after emplacement of the host basalt have little to no effect on the total water content of pyroxenes. Second, the study of the xenoliths from the pyroclastic deposit at Ray Pic reveals that the water concentration of olivine and pyroxenes is strongly influenced by the degree of degassing of the magma before or during the eruption and may vary throughout the entire eruptive sequence. However, the infrared spectral signatures of pyroxenes are not impacted by late degassing, and different spectral signatures can coexist within the same magma and the same eruption products.

To date, no solid, straight correlation between major element composition and water content in mantle pyroxenes has been found (see, for instance, Peslier, 2010). This may be explained by the impact of degassing on the final values of OH defects in olivine but also in pyroxenes. Another consequence is that the water content of pyroxenes in mantle xenoliths represents only a fraction of their water content before the degassing of magma and can only be used to estimate a minimum water content of pyroxenes before degassing.

Code and data availability. Calculations and graphs have been made using the free software GNU Octave. Datasets are provided in the Supplement.

Supplement. The supplement related to this article is available online at https://doi.org/10.5194/ejm-38-477-2026-supplement.

Author contributions. JI conceptualized the research, obtained the funding, and administrated and supervised the research activity. KT carried out the analyses, developed the code for the data analysis, and performed the data processing. KT wrote the first draft, and JI and KT wrote the final version, with input from ED, LF, and HC. The fieldwork of 2020 was carried out by JI, KT, ED, and LF; the fieldwork of 2016 was carried out by JI, ED, and HC.

Competing interests. At least one of the (co-)authors is a member of the editorial board of *European Journal of Mineralogy*. The peer-review process was guided by an independent editor, and the authors also have no other competing interests to declare.

Disclaimer. Publisher's note: Copernicus Publications remains neutral with regard to jurisdictional claims made in the text, published maps, institutional affiliations, or any other geographical representation in this paper. The authors bear the ultimate responsibil-

ity for providing appropriate place names. Views expressed in the text are those of the authors and do not necessarily reflect the views of the publisher.

Acknowledgements. Isabelle De Waele is acknowledged for providing help during FTIR sessions at LASIRe, Lille. Maria Drouka is thanked for the analysis of the Burz16 02 sample. We thank Jérôme Perrachon of the Carrières Perrachon Jean Léon SAS for allowing us the access to the Ringue quarry. We are grateful to Jin Lu, Changze He, and Chenghao Wang, students from the Zhejiang University's School of Earth Sciences, who reviewed an early draft of this work. Monika Koch-Müller, two anonymous reviewers, and the EJM associate editor are thanked for their constructive comments.

Financial support. Part of the work was supported by the SYSTER Program of CNRS-INSU 2019, attributed to JI. The PhD thesis of KT was granted by the University of Lille.

Review statement. This paper was edited by Dejan Prelević and reviewed by Monika Koch-Müller and two anonymous referees.

References

Azevedo-Vannson, S., France, L., Ingrin, J., and Chazot, G.: Mantle metasomatic influence on water contents in continental lithosphere: New constraints from garnet pyroxenite xenoliths (France & Cameroon volcanic provinces), Chem. Geol., 575, 120257, https://https://doi.org/10.1016/j.chemgeo.2021.120257, 2021.

Bell, D. R. and Rossman, G. R.: Water in the Earth's mantle: the role of nominally anhydrous minerals, Science, 255, 1391–1397, https://doi.org/10.1126/science.255.5050.1391, 1992.

Bell, D. R., Ihinger, P. D., and Rossman, G. R.: Quantitative analysis of trace OH in garnet and pyroxenes, Am. Mineral., 80, 465–474, https://doi.org/10.2138/am-1995-5-607, 1995.

Bräuer, K., Kämpf, H., Niedermann, S., and Wetzel, H.-U.: Regional distribution pattern of carbon and helium isotopes from different volcanic fields in the French Massif Central: Evidence for active mantle degassing and water transport, Chem. Geol., 469, 4–18, https://doi.org/10.1016/j.chemgeo.2017.04.004, 2017.

Brey, G. P. and Köhler, T.: Geothermobarometry in four-phase lherzolites II. New thermobarometers, and practical assessment of existing thermobarometers, J. Petrol., 31, 1353–1378, https://doi.org/10.1093/petrology/31.6.1353, 1990.

Carignan, J., Hild, P., Mevelle, G., Morel, J., and Yeghicheyan, D.: Routine analyses of trace elements in geological samples using flow injection and low pressure on-line liquid chromatography coupled to ICP-MS: A study of geochemical reference materials BR, DR-N, UB-N, AN-G and GH, Geostandards Newsletter, Journal of Geostandards and Geoanalysis, 25, 187–198, https://doi.org/10.1111/j.1751-908X.2001.tb00595.x, 2001.

Chen, H., Xia, Q.-K., Ingrin, J., Jia, Z.-B., and Feng, M.: Changing recycled oceanic components in the mantle source of the Shuangliao Cenozoic basalt, NE China: New constraints from water content, Tectonophysics, 650, 113–123, https://doi.org/10.1016/j.tecto.2014.07.022, 2015.

Della Ventura, G., Hawthorne, F. C., Robert, J. L., and Iezzi, D.: Synthesis and infrared spectroscopy of amphiboles along the tremolite-pargasite join, Europ. J. Mineral., 15, 341–347, https://doi.org/10.1127/0935-1221/2003/0015-0341, 2003.

Demers-Roberge, A., Jollands, M. C., Tollan, P., and Müntener, O.: H diffusion in orthopyroxene and the retention of mantle water signatures, Geochim. Cosmochim. Ac., 305, 263–281, https://doi.org/10.1016/j.gca.2021.04.005, 2021.

Demers-Roberge, A., Jollands, M. C., and Müntener, O.: Hydrogen incorporation in orthopyroxene from Southern Patagonia mantle xenoliths: the role of cooling upon emplacement, Am. Mineral., https://doi.org/10.2138/am-2025-9798, 2026.

Demouchy, S. and Bolfan-Casanova, N.: Distribution and transport of hydrogen in the lithospheric mantle: A review, Lithos, 240–243, 402–425, https://doi.org/10.1016/j.lithos.2015.11.012, 2016.

Demouchy, S., Jacobsen, S. D., Gaillard, F., and Stern, C. R.: Rapid magma ascent recorded by water diffusion profiles in olivine from Earth's mantle, Geology, 34, 429–432, https://doi.org/10.1130/G22386.1, 2006.

Denis, C., Demouchy, S., and Shaw, C.: Evidence of dehydration in peridotites from Eifel Volcanic Field and estimates of the rate of magma ascent, J. Volcanol. Geotherm. Res., 258, 85–99, https://doi.org/10.1016/j.jvolgeores.2013.04.010, 2013.

Denis, C. M. M., Alard, O., and Demouchy, S.: Water content and hydrogen behaviour during metasomatism in the uppermost mantle beneath Ray Pic volcano (Massif Central, France), Lithos, 236–237, 256–274, https://doi.org/10.1016/j.lithos.2015.08.013, 2015.

Denis, C. M. M., Demouchy, S., and Alard, O.: Heterogeneous hydrogen distribution in orthopyroxene from veined mantle peridotite (San Carlos, Arizona): Impact of melt-rock interactions, Lithos, 302–303, 298–311, https://doi.org/10.1016/j.lithos.2018.01.007, 2018.

Downes, H. and Dupuy, C.: Textural, isotopic and REE variations in spinel peridotite xenoliths, Massif Central, France, Earth Plane. Sc. Lett., 82, 121–135, https://doi.org/10.1016/0012-821X(87)90112-9, 1987.

Farver, J. R.: Oxygen and hydrogen diffusion in minerals, Rev. Mineral. Geochem., 72, 447–507, https://doi.org/10.2138/rmg.2010.72.10, 2010.

Elms, H. C., Myers, M. L., Nichols, A. R. L., Wallace, P. J., Wilson, C. J. N., Barker, S. J., and Charlier, B. L. A.: Pre-eruptive rhyolite magma ascent rate is rapid and independent of eruption size: a case study from Ōkataina Volcanic Centre, Aotearoa New Zealand, Bull. Volcanol., 85, 20, https://doi.org/10.1007/s00445-023-01630-7, 2023.

Ferriss, E., Plank, T., and Walker, D.: Site-specific hydrogen diffusion rates during clinopyroxene dehydration, Contrib. Mineral. Petrol., 171, 55, https://doi.org/10.1007/s00410-016-1262-8, 2016.

Grant, K., Ingrin, J., Lorand, J. P., and Dumas, P.: Water partitioning between mantle minerals from peridotite xenoliths, Contrib. Mineral. Petrol., 154, 15–34, https://doi.org/10.1007/s00410-006-0177-1, 2007.

Gu, X.: Melt-rock interaction signatures in peridotite from sub-continental mantle (French Massif Central): A trace

element, H, Li and $\square^7$Li approach, Earth Sciences, Université de Lorraine, English, (NNT: 2016LORR0052), https://doi.org/10.70675/b08ad0aczfea8z47ddz913czfe7d400fa1e1, 2016.

Gu, X., Deloule, E., France, L., and Ingrin, J.: Multi-stage metasomatism revealed by trace element and Li isotope distributions in minerals of peridotite xenoliths from Allègre volcano (French Massif Central), Lithos, 264, 158–174, https://doi.org/10.1016/j.lithos.2016.07.019, 2016.

Harvey, J., Gannoun, A., Burton, K. W., Schiano, P., Rogers, N. W., and Alard, O.: Unravelling the effects of melt depletion and secondary infiltration on mantle Re–Os isotopes beneath the French Massif Central, Geochim. Cosmochim. Ac., 74, 293–320, https://doi.org/10.1016/j.gca.2009.09.031, 2010.

Hauri, E. H., Gaetani, G. A., and Green, T. H.: Partitioning of water during melting of the Earth's upper mantle at H_2O-undersaturated conditions, Earth Planet. Sc. Lett., 248, 715–734, https://doi.org/10.1016/j.epsl.2006.06.014, 2006.

Ingrin, J., Latrous, K., Doukhan, J., and Doukhan, N.: Water in diopside: an electron microscopy and infrared spectroscopy study, Eur. J. Mineral., 1, 327–342, https://doi.org/10.1127/ejm/1/3/0327, 1989.

Ingrin, J. and Blanchard, M.: Diffusion of hydrogen in minerals, in: Reviews in Mineralogy and Geochemistry, edited by: Keppler, H. and Smyth, J. R., Washington, D. C., Mineral. Soc. Am., 62, 291–320, https://doi.org/10.2138/rmg.2006.62.13, 2006.

Ingrin, J. and Skogby, H.: Hydrogen in nominally anhydrous upper-mantle minerals: concentration levels and implications, Eur. J. Mineral., 12, 543–570, https://doi.org/10.1127/ejm/12/3/0543, 2000.

Ju, D., Du, W., Liu, Z., Chen, L., and Yu, W.: Initial Water Content in Pyroxenes Constrained by Experimental and Numerical Simulations: Reassessment of Clinopyroxene as a Standard for Estimating Water Content in the Earth's Upper Mantle, J. Geophys. Res. Solid Earth, https://doi.org/10.1029/2025JB031788, 2025.

Kovács, I., Hermann, J., O'Neill, H. S. C., Gerald, J. F., Sambridge, M., and Horváth, G.: Quantitative absorbance spectroscopy with unpolarized light: Part II. Experimental evaluation and development of a protocol for quantitative analysis of mineral IR spectra, Am. Mineral., 93, 765–778, https://doi.org/10.2138/am.2008.2656, 2008.

Ledru, P., Vitel, G., Marchand, J., Maurin, G., Mercier, F., Turland, M., Etlicher, B., Dautria, J. M., and Liotard, J. M.: Notice explicative, Carte géol. France (1/50000), feuille Craponne-sur-Arzon (767), Orléans, BRG M, Carte géologique par P. Ledru et al., 74 pp., ISBN 2-7159-1767-8, 1994.

Lenoir, X., Garrido, C. J., Bodinier, J.-L., and Dautria, J.-M.: Contrasting lithospheric mantle domains beneath the Massif Central (France) revealed by geochemistry of peridotite xenoliths, Earth Planet. Sc. Lett., 181, 359–375, https://doi.org/10.1016/S0012-821X(00)00216-8, 2000.

Li, Z.-Y., Wang, Y.-F., and Zhang, J.-F.: Hydrogen loss from pyroxene within granulite xenoliths at Damaping, North China craton, J. Asian Earth Sci., 276, https://doi.org/10.1016/j.jseaes.2024.106331, 2024.

Libowitzky, E. and Rossman, G. R.: An IR absorption calibration for water in minerals, Am. Mineral., 82, 1111–1115, https://doi.org/10.2138/am-1997-11-1208, 1997.

Liu, J., Xia, Q-K., Deloule, E., Ingrin, J., Chen, H., and Feng, M.: Water content and oxygen isotopic composition of alkali basalts from the Taihang mountains, China: Recycled oceanic components in the mantle source, J. Petrol., 56, 681–702, https://doi.org/10.1093/petrology/egv013, 2015.

Maury, R. C. and Varet, J.: Le volcanisme tertiaire et quaternaire en France, 107 Éditions du BRGM, 137–159, ISBN 2-7159-5011-X, 1980.

Mercier, J.-C. C. and Nicolas, A.: Textures and fabrics of upper-mantle peridotites as illustrated by xenoliths from basalts, J. Petrol., 16, 454–487, 1975.

Michon, L. and Merle, O.: The evolution of the Massif Central Rift; spatio-temporal distribution of the volcanism, Bulletin de la Société Géologique de France, 172, 201–211, https://doi.org/10.2113/172.2.201, 2001.

Moussallam, Y., Rose-Koga, E. F., Koga, K. T., Médard, E., Bani, P., Devidal, J.-L., and Tari, D.: Fast ascent rate during the 2017–2018 Plinian eruption of Ambae (Aoba) volcano: a petrological investigation, Contrib. Mineral. Petrol., 174, 90–203, https://doi.org/10.1007/s00410-019-1625-z, 2019.

O'Leary, J. A., Gaetani, G. A., and Hauri E. H.: The effect of tetrahedral Al^{3+} on the partitioning of water between clinopyroxene and silicate melt, Earth Planet. Sc. Lett., 297, 111–120, https://doi.org/10.1016/j.epsl.2010.06.011, 2010.

Patkó, L., Liptai, N., Kovács, I., Aradi, L., Xia, Q., Ingrin, J., Mihály, J., O'Reilly, S., Griffin, W., Wesztergom, V., and Szabó, C.: Extremely low structural hydroxyl contents in upper mantle xenoliths from the Nógrád-Gömör Volcanic Field (northern Pannonian Basin): Geodynamic implications and the role of post-eruptive re-equilibration, Chem. Geol., 507, 23–41, https://doi.org/10.1016/j.chemgeo.2018.12.017, 2019.

Peck, D. L.: Cooling and vesiculation of Alae Lava Lake, Hawaii, Professional Paper 935-B, US Govt. Print. Off., https://doi.org/10.3133/pp935B, 1978.

Peslier, A. H. and Luhr, J. F.: Hydrogen loss from olivines in mantle xenoliths from Simcoe (USA) and Mexico: mafic alkalic magma ascent rates and water budget of the subcontinental lithosphere, Earth Planet. Sc. Lett., 242, 302–319, https://doi.org/10.1016/j.epsl.2005.12.019, 2006.

Peslier, A. H.: A review of water contents of nominally anhydrous natural minerals in the mantles of Earth, Mars and the Moon, J. Volcanol. Geotherm. Res., 197, 239–258, https://doi.org/10.1016/j.jvolgeores.2009.10.006, 2010.

Peslier, A. H., Schönbächler, M., Busemann, H., and Karato, S. I.: Water in the Earth's Interior: Distribution and Origin, Space Sci. Rev., 212, 743–810, https://doi.org/10.1007/s11214-017-0387-z, 2017.

Philpotts, A. and Ague, J.: Cooling of igneous bodies and other diffusion processes, Principles of Igneous and Metamorphic Petrology, Cambridge University Press, 111-129, https://doi.org/10.1017/CBO9780511813429, 2018.

Shaw, H. R., Hamilton, M. S., and Peck, D. L.: Numerical analysis of lava lake cooling models; Part I, Description of the method, Am. J. Sci., 277, 384–414, https://doi.org/10.2475/ajs.277.4.384, 1977.

Skogby, H., Bell, D. R., and Rossman G. R.: Hydroxide in pyroxene; variations in the natural environment, Am. Mineral., 75, 764–774, 1990.

Tian, Z., Liu, J., Xia, Q., Ingrin, J., Hao, Y., and Christophe, D.: Water concentration profiles in natural mantle orthopyroxenes: A geochronometer for long annealing of xenoliths within magma, Geology, 45, 87–90, https://doi.org/10.1130/G38620.1, 2017.

Uenver-Thiele, L., Woodland, A. B., Seitz, H.-M., Downes, H., and Altherr, R.: Metasomatic Processes Revealed by Trace Element and Redox Signatures of the Lithospheric Mantle Beneath the Massif Central, France, J. Petrol., 58, 395–422, https://doi.org/10.1093/petrology/egx020, 2017.

Withers, A. C., Bureau, H., Raepsaet, C., and Hirschmann, M. M.: Calibration of infrared spectroscopy by elastic recoil detection analysis of H in synthetic olivine, Chem. Geol., 334, 92–98, https://doi.org/10.1016/j.chemgeo.2012.10.002, 2012.

Wittig, N., Baker, J. A., and Downes, H.: U–Th–Pb and Lu–Hf isotopic constraints on the evolution of sub-continental lithospheric mantle, French Massif Central, Geochim. Cosmochim. Ac., 71, 1290–1311, https://doi.org/10.1016/j.gca.2006.11.025, 2007.

Wittmann, W., Sigmundsson, F., Dumont, S., and Lavallée, Y.: Post-emplacement cooling and contraction of lava flows: InSAR observations and a thermal model for lava fields at Hekla volcano, Iceland, J. Geophys. Res.-Sol, Ea,, 122, 946–965, https://doi.org/10.1002/2016JB013444, 2017.

Xia, Q.-K., Liu, J., Liu, S.-C., Kóvacs, I., Feng, M., and Dang, L.: High water content in Mesozoic primitive basalts of the North China Craton and implications on the destruction of cratonic mantle lithosphere, Earth Planet. Sc. Lett., 361, 85–97, https://doi.org/10.1016/j.epsl.2012.11.024, 2013.

Yang, Y., Ingrin, J., Liu, W., Huang, W., Gu, X., and Xia Q.-K.: Behavior and origin of hydrogen defects in natural orthopyroxene during high-temperature processes, Am. Mineral., 106, 1768–1779, https://doi.org/10.2138/am-2021-7741, 2021.

Zangana, N. A., Downes, H., Thirlwall, M. F., and Hegner, E.: Relationship between deformation, equilibration temperatures, REE and radiogenic isotopes in mantle xenoliths (Ray Pic, Massif Central, France): an example of plume–lithosphere interaction?, Contrib. Mineral. Petrol., 127, 187–203, https://doi.org/10.1007/s004100050275, 1997.

Zangana, N. A., Downes, H., Thirlwall, M., Marriner, G., and Bea, F.: Geochemical variation in peridotite xenoliths and their constituent clinopyroxenes from Ray Pic (French Massif Central): implications for the composition of the shallow lithospheric mantle, Chem. Geol., 153, 11–35, https://doi.org/10.1016/S0009-2541(98)00150-8, 1999.